PADINA PAVONICA ETHANOL EXTRACT TRIGGERS APOPTOSIS AND CELL CYCLE DISRUPTION THROUGH REDOX STRESS AND PI3K/AKT MODULATION IN LUNG AND BREAST CARCINOMA CELLS

Khulud M. Alshehri
Department of Biology, Faculty of Science, Al-Baha University, Al-Baha 65527, Saudi Arabia
Email: kalshehri@bu.edu.sa

Abstract

Background: Marine brown algae contain bioactive compounds with anti-cancer properties. *Padina pavonica* (PP), a common brown alga, remains understudied for cancer cell effects. This study evaluated the cytotoxic and molecular effects of ethanol extract versus cisplatin (CP) on human lung carcinoma (A549) and breast carcinoma (MCF-7) cells.

Methods: The SRB test was used to determine cell toxicity by determining the IC_{50} values. After treatment with Padina pavonica (PP) extract and cisplatin (CP), cell shape changes were observed microscopically. A FLUOstar Omega microplate reader was used to measure cellular glutathione (GSH) and total antioxidant capacity. Flow cytometry with Annexin V/PI staining and PI DNA analysis was used to assess cell death and cell cycle progression. RT-qPCR measured Bax, Bcl-2, PI3K, and AKT1 gene expression, while western blotting confirmed the protein levels. One-way ANOVA with Tukey's test was used to check for statistical significance.

Results: *Padina pavonica* extract reduced cell viability in a dose-dependent manner, with IC50 values of 60.73 µg/mL in A549 and 173.11 µg/mL in MCF-7, versus 1.32 µg/mL and 1.72 µg/mL for cisplatin (CP), respectively. Morphological analysis showed cytotoxic features, including shrinkage, rounding, and detachment. PP treatment depleted intracellular glutathione (GSH) and reduced antioxidant capacity, indicating disrupted redox homeostasis; depletion was partial in A549 cells but profound in MCF-7 cells. Flow cytometry revealed that PP induced late apoptosis in A549 cells and late apoptosis/necrosis in MCF-7 cells, whereas CP triggered both early and late apoptosis. Cell cycle analysis showed that PP caused G1 arrest in A549 cells and sub-G1 accumulation in MCF-7 cells, whereas CP increased the sub-G1 population. RT-qPCR showed upregulation of Bax and downregulation of Bcl-2, PI3K, and AKT1 in A549 cells, while MCF-7 cells showed reduced Bcl-2 and AKT1 but increased PI3K. Western blotting validated these changes at the protein level, confirming PP as a modulator of apoptotic pathways.

Conclusion: *Padina pavonica* extract exhibits anticancer activity by reducing cell viability, altering morphology, depleting glutathione, lowering antioxidant capacity, and disrupting redox homeostasis. These effects induce apoptosis and cell cycle arrest and modulate PI3K/AKT signaling, with stronger responses in A549 versus MCF-7 cells. Although less potent than cisplatin, PP extract impaired survival pathways through layered mechanisms. These findings highlight the potential of marine brown algae as anticancer agents.

Keywords: A549, MCF-7, *Padina pavonica*, Apoptosis, PI3K/AKT signaling pathway, Oxidative stress.

1. Introduction

Cancer remains one of the leading causes of morbidity and mortality worldwide, with lung and breast cancers representing two of the most prevalent and fatal malignancies (Sung *et al*., 2021). Lung

Gland Surg
VOL-11 NO 1 (2026)
ISSN:2227-684X | E-ISSN:2227-8575

cancer, particularly non-small cell lung carcinoma (NSCLC), accounts for approximately 85% of all lung cancer cases and continues to show poor survival rates despite advances in targeted therapies and immunotherapy. Breast cancer, on the other hand, is the most frequently diagnosed cancer among women globally, with hormone receptor-positive subtypes such as MCF-7 serving as widely used experimental models (Kim *et al*., 2025). Conventional chemotherapeutic agents, including cisplatin, remain central to treatment regimens but are often limited by severe toxicity, drug resistance, and lack of selectivity toward malignant cells (Galluzzi *et al*., 2012). These challenges underscore the urgent need for novel therapeutic agents that are both effective and less harmful to normal tissues (Pradhan *et al*., 2023).

Natural products have historically been a rich source of bioactive compounds for cancer therapy (El-Seedi *et al*., 2025). Plant-derived molecules such as paclitaxel and vincristine, as well as marine-derived compounds such as trabectedin, highlight the potential of natural sources to yield clinically relevant anticancer drugs (Tamzi *et al*., 2024). Marine organisms are increasingly recognized as reservoirs of structurally diverse metabolites with unique pharmacological properties (Pradhan *et al*., 2023). Marine algae, or seaweeds, have attracted attention due to their abundance, ecological sustainability, and broad spectrum of biological activities, including antioxidant, anti-inflammatory, antimicrobial, and anticancer effects (El-Seedi *et al*., 2025). Brown algae (Phaeophyceae) are especially notable for their secondary metabolites, such as phlorotannins, fucoidans, and sterols, which have been implicated in modulating key cellular pathways involved in cancer progression (Luo *et al*., 2023).

Padina pavonica, a brown alga widely distributed on the Mediterranean and Atlantic coasts, has been traditionally studied for its nutritional and ecological roles (Bernardini *et al*., 2018). Recent phytochemical analyses have revealed that *P. pavonica* contains bioactive compounds, including terpenoids, flavonoids, phenolic acids, and sulfated polysaccharides (Makhlof *et al*., 2024). Preliminary studies have demonstrated the antioxidant, antimicrobial, and cytotoxic activities of these metabolites (Catarino et al. 2021). Importantly, extracts of *P. pavonica* have been reported to exert antiproliferative effects on various cancer cell lines, suggesting their potential utility as a source of anticancer agents (Bernardini *et al*., 2018). However, systematic investigations into its mechanisms of action, particularly in relation to apoptosis, cell cycle regulation, and signaling pathways, remain limited (Muñoz-Losada *et al*., 2025).

Apoptosis or programmed cell death is a critical mechanism by which anticancer agents exert their effects (Santhanam *et al*., 2024). Dysregulation of apoptotic pathways, including the balance between pro-apoptotic (Bax) and anti-apoptotic (Bcl-2) proteins, contributes to cancer cell survival and resistance to therapy (Luo *et al*., 2023). Similarly, aberrant activation of the PI3K/AKT/mTOR signaling pathway promotes cell proliferation, survival, and metabolic reprogramming in many cancers, including lung and breast carcinomas (Muñoz-Losada *et al*., 2025). Targeting these pathways has emerged as a promising strategy for overcoming resistance and improving therapeutic outcomes (Tamzi *et al*., 2024). Therefore, natural products capable of modulating Bax/Bcl-2 expression and inhibiting PI3K/mTOR signaling may represent valuable candidates for anticancer drug development (Catarino *et al*., 2021).

Cisplatin, a platinum-based chemotherapeutic agent, is widely used as a reference drug in experimental oncology owing to its well-characterized cytotoxic and pro-apoptotic effects (Dasari and

Gland Surg
VOL-11 NO 1 (2026)
ISSN:2227-684X | E-ISSN:2227-8575

Bernard Tchounwou, 2014). Its mechanism of action involves DNA cross-linking, generation of reactive oxygen species, and activation of intrinsic apoptotic pathways (Galluzzi *et al*., 2012). Despite its efficacy, cisplatin is associated with nephrotoxicity, neurotoxicity, and the development of resistance in many tumors (Yılmaz *et al*., 2023). Comparing the activity of natural extracts, such as *P. pavonica*, with cisplatin provides a benchmark for evaluating their relative potency and mechanistic overlap, while also highlighting potential advantages in terms of reduced toxicity or novel pathway modulation (Makhlof *et al*., 2024; Palpperumal *et al*., 2024).

Given the global burden of lung and breast cancers and the limitations of current chemotherapeutic agents, there is a compelling need to explore alternative sources of anticancer compounds (Kim *et al*., 2025). Marine algae such as *Padina pavonica* represent underexplored reservoirs of bioactive metabolites with the potential to modulate key cancer-related pathways (Palpperumal *et al*., 2024). Preliminary evidence suggests that *P. pavonica* extracts may exert cytotoxic and pro-apoptotic effects, but comprehensive studies across multiple cancer cell lines with mechanistic validation are scarce (Palpperumal *et al*., 2024). Furthermore, direct comparisons with established chemotherapeutics, such as cisplatin, are necessary to contextualize the therapeutic relevance of these natural extracts (Elmorsy *et al*., 2024).

The present work investigated the anticancer potential of *Padina pavonica* extract in two distinct human cancer cell lines: A549 (lung carcinoma) and MCF-7 (breast carcinoma). Using cisplatin as a reference drug, we evaluated the extract's effects on cell viability and morphological alterations, followed by assessments of apoptosis and cell cycle progression. Molecular analyses included gene and protein expression profiling of Bax, Bcl-2, PI3K, and AKT1 to elucidate the apoptotic and survival signaling pathways. In addition, intracellular glutathione (GSH) levels and total antioxidant capacity were measured to determine the impact of the extract on redox homeostasis, providing further insight into oxidative stress as a complementary mechanism of cytotoxicity. By integrating cytotoxic, molecular, and biochemical evidence across the two cancer models, this study offers a comprehensive evaluation of *P. pavonica* as a promising source of novel anticancer agents.

2. Material and Methods

2.1. Standard Preparation

An aliquot was extracted from a stock solution that included ten reference standards: Gallic acid, Rutin, Chlorogenic acid, Catechin, Ellagic acid, Quercetin, Kaempferol, Apigenin, Hesperidin, and Caffeic acid, each at a concentration of 1 mg/mL. Working solutions were prepared from this stock with a final concentration of 10 µg/mL for each standard. Subsequently, 20 µL of each solution was injected into the HPLC system for analysis.

2.2. Sample Preparation

To prepare the solutions, 55 mg of Tur_Orn extract and 46.7 mg of Sur_Flu extract were each dissolved in 1 mL of methanol, resulting in concentrations of 55 mg/mL and 46.7 mg/mL, respectively. These solutions were then thoroughly mixed using a vortex and sonicated for 15 min to ensure they were completely dissolved. After sonication, each solution was filtered through a 0.45 µm PTFE syringe filter to eliminate any particulates. The filtered solutions were directly injected into the HPLC system for analysis.

2.3. Chromatographic Condition

Gland Surg
VOL-11 NO 1 (2026)
ISSN:2227-684X | E-ISSN:2227-8575

<table>
<tr><td>Instrument:</td><td>Waters 2690 Alliance HPLC system equipped with a Waters 996 photodiode array detector.</td></tr>
<tr><td>Mobile Phase:</td><td>0.1% Orthophosphoric acid: Methanol (Gradient method)
<table>
<tr><th>Time (min)</th><th>Orthophosphoric acid 0.1%</th><th>Methanol</th></tr>
<tr><td>0</td><td>95</td><td>5</td></tr>
<tr><td>3</td><td>95</td><td>5</td></tr>
<tr><td>50</td><td>50</td><td>50</td></tr>
<tr><td>55</td><td>30</td><td>70</td></tr>
<tr><td>75</td><td>10</td><td>90</td></tr>
<tr><td>76</td><td>95</td><td>5</td></tr>
<tr><td>80</td><td>95</td><td>5</td></tr>
</table></td></tr>
<tr><td>Column:</td><td>KromasilC_{18} (5µm,4.6 x 250mm)</td></tr>
<tr><td>Column Temperature:</td><td>25° C</td></tr>
<tr><td>Autosampler Temperature:</td><td>Ambient</td></tr>
<tr><td>Flow Rate:</td><td>1 mL/min</td></tr>
<tr><td>Wavelength:</td><td>280 nm</td></tr>
<tr><td>Injection Volume:</td><td>50 µL</td></tr>
<tr><td>Run Time:</td><td>80 min</td></tr>
</table>

2.4. Cell culture

Human lung cancer cells (A549) and breast cancer cells (MCF-7) were sourced from Nawah Scientific Inc., located in Mokatam, Cairo, Egypt. The A549 cell line was grown in RPMI medium, whereas the MCF-7 cell line was cultured in DMEM. Both media were enriched with 100 mg/mL streptomycin, 100 U/mL penicillin, and 10% heat-inactivated fetal bovine serum. The cell cultures were maintained at 37 °C in a humidified environment with 5% CO2 (Abuwatfa *et al*., 2024).

2.5. Cytotoxicity assay

The sulforhodamine B (SRB) assay was used to assess cell viability. Briefly, A549 and MCF-7 cells were plated in 96-well plates at a concentration of 5×10^3 cells per well and allowed to adhere for 24 h. Subsequently, the cells were exposed to different concentrations of the Padina pavonica extract or cisplatin. Following treatment, the cells were fixed with 10% (w/v) trichloroacetic acid (TCA) for 1 h at 4 °C, rinsed, and stained with a 0.4% (w/v) SRB solution for 10 min in the dark. Excess dye was removed using 1% (v/v) acetic acid, and the dye bound to the proteins was dissolved in 10 mM Tris base (pH ~10.5). Absorbance was recorded at 540 nm using an Infinite F50 microplate reader (TECAN, Switzerland). Cell viability was calculated as a percentage compared to untreated controls, and IC_{50} values were determined (Kouroshnia *et al*., 2022).

2.6. Morphological assessment

Microscopic examination was conducted to observe morphological changes following treatment with varying concentrations of *Padina pavonica* extract (10, 100, and 1000 µg/ml) or cisplatin. Cells that did not receive any treatment were used as controls. Documented structural changes include cell shrinkage, rounding, detachment, and disruption of monolayer integrity. (Sali *et al*., 2024).

2.7. Apoptosis analysis (Annexin V/PI flow cytometry)

To quantify apoptotic cell populations, an Annexin V-FITC/PI apoptosis detection kit from Abcam (UK) was used. Following treatment, 1×10^5 cells were collected, rinsed twice with PBS, and

Gland Surg
VOL-11 NO 1 (2026)
ISSN:2227-684X | E-ISSN:2227-8575

then incubated with an Annexin V-FITC/PI solution for 30 min at room temperature in the absence of light. The samples were examined using a NovoCyte™ flow cytometer (ACEA Biosciences, USA), with FITC and PI emissions recorded at λ_ex/em = 488/530 nm and 535/617 nm, respectively. A minimum of 12,000 events were gathered per sample, and quadrant analysis was conducted using NovoExpress™ software (Li *et al*., 2025).

2.8. Cell cycle analysis (PI staining)

To assess the cell cycle activities, 1 × 10^5 A549 and MCF-7 cells that had been treated were fixed in 60% ice-cold ethanol at 4 °C for one hour. The cells were then washed and resuspended in PBS containing 50 µg/mL RNase A and 10 µg/mL propidium iodide (PI). The cells were then incubated for 20 min at 37 °C in the dark, after which their DNA content was examined using flow cytometry (NovoCyte™, ACEA Biosciences). At least 12,000 events were recorded for each sample, and the cell cycle distribution was determined using NovoExpress™ software. (Kouroshnia *et al*., 2022).

2.9. Total antioxidant capacity assay

The total antioxidant capacity was assessed using a Biodiagnostic kit available commercially in Egypt. This assay measures the ability of antioxidants in a sample to neutralize added hydrogen peroxide (H2O2), thereby preventing the formation of a colored oxidation product. The absorbance was then recorded at 505 nm using a FLUOstar Omega microplate reader from BMG Labtech, Germany (Silvestrini *et al*., 2023).

2.10. Glutathione (GSH) assay

The intracellular reduced glutathione (GSH) levels were evaluated using a biodiagnostic kit from Egypt. This method relies on GSH's ability of GSH to reduce 5,5′-dithiobis (2-nitrobenzoic acid) (DTNB), leading to the production of the yellow chromophore 5-thio-2-nitrobenzoic acid (TNB). The chromophore intensity was measured spectrophotometrically at 405 nm using a FLUOstar Omega microplate reader from BMG Labtech, Germany (Kalinina, 2024).

2.11. Gene expression analysis (qRT-PCR)

Total RNA was isolated using an RNeasy Mini Kit (Qiagen, Germany), and its concentration and purity were verified spectrophotometrically by assessing the A260/280 ratio. Two micrograms of RNA was converted into cDNA using the RevertAid First Strand cDNA Synthesis Kit (Thermo Scientific, Lithuania). Quantitative PCR was performed using SYBR Green Master Mix (Qiagen) on a Bio-Rad CFX Opus 96 system. Each 20 µL reaction mixture comprised 2 µL cDNA, 0.3–0.5 µM primers, 10 µL master mix, and nuclease-free water. The target genes included Bax, Bcl-2, PI3K, and AKT1, with GAPDH serving as a housekeeping control (Li *et al*., 2025).

2.12. Protein expression analysis (Western blot)

Cells were lysed using RIPA buffer with added protease and phosphatase inhibitors. The lysates were then clarified by centrifugation, and the total protein content was measured using the BCA assay. Equal amounts (20–50 µg) of proteins were separated by SDS-PAGE and transferred to PVDF membranes. The membranes were blocked with 5% skimmed milk in TBST, incubated overnight at 4 °C with primary antibodies, washed, and then treated with HRP-conjugated secondary antibodies. Bands were detected using an enhanced chemiluminescence (ECL) substrate (Thermo Scientific) and captured on a Bio-Rad system. The intensity of the bands was analyzed by densitometry using an image analysis software (Mahmood and Yang, 2012).

Gland Surg
VOL-11 NO 1 (2026)
ISSN:2227-684X | E-ISSN:2227-8575

2.13. Statistical analysis

All experiments were conducted in triplicate, and the results are expressed as the mean ± SEM. Statistical significance, determined by one-way ANOVA followed by Tukey's post-hoc test, was defined as *p< 0.05. The following symbols were used to denote significance: *p < 0.05, **p < 0.01, ***p < 0.001, and ****p < 0.0001; ns indicates not significant (McDonald, 2014).

3. Results

3.1. GC-MS Assessment

As shown in **Figure 1** and **Table 1**, the *Padina pavonica* extract exhibited a chemically diverse volatile fraction dominated by long-chain fatty acids and their esters, sterols, and terpenoid- or phenolic-derived derivatives (Sudha and Balasundaram, 2018; Shahin *et al*., 2022). Polyunsaturated C18–C22 fatty acids such as arachidonic acid, oleic/linoleic acid isomers, and their methyl and ethyl esters constituted a major proportion of the chromatographic area, reflecting a lipid-rich profile typical of brown macroalgae and suggesting potential anti-inflammatory- and cardioprotective properties. Mono- and polyhydroxylated fatty acid esters (e.g., 2,3-dihydroxypropyl palmitate, linolenic acid 2-hydroxy-1-(hydroxymethyl)ethyl ester) were also detected and are consistent with the reported roles of glycolipid-type constituents in membrane architecture and bioactivity in marine algae.

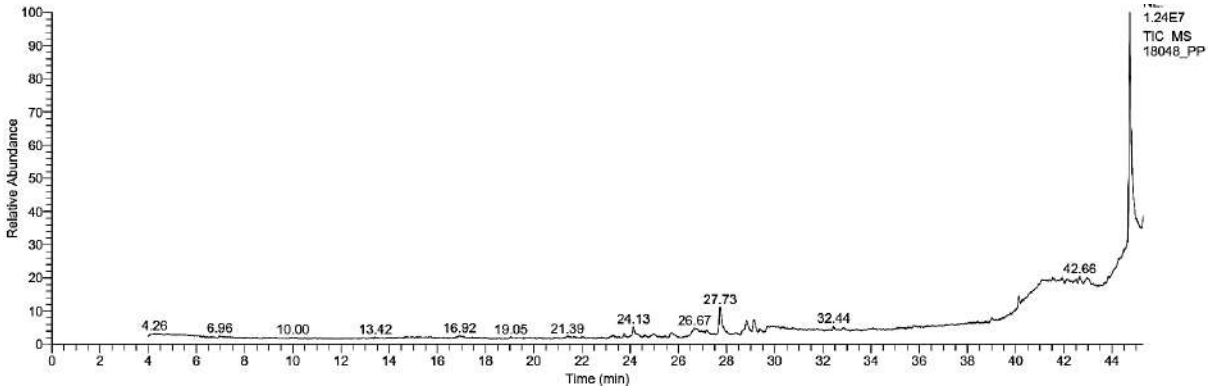

Figure 1. GC–MS of *Padina pavonica* extract.

The GC–MS data further revealed several epoxy, acetylenic, and trienoic fatty acids (e.g., 1,2-15,16-diepoxyhexadecane, 17-octadecynoic acid, and 7,10,13-eicosatrienoic acid methyl ester), indicating that oxidative and enzymatic transformations of unsaturated lipids contribute to the volatile chemical space of *P. pavonica* (Jerković *et al*., 2019). A substantial sterol fraction, dominated by cholest-5-en-3-ol derivatives, stigmasta-5,24(28)-dien-3-ol, and various pregnane-type steroids, accounted for the largest single peak at RT 44.73 min, underscoring the importance of Δ5^{5}5-sterols and related nuclei in the algal metabolome and aligning with previous reports of sterol-mediated cytoprotective and cholesterol-lowering effects in brown seaweeds. In addition, silicon-derivatized phenolics and sugars (e.g., thymol and carvacrol TBDMS derivatives, arabinitol pentaacetate, and galactopyranoside trimethylsilyl boronates) were observed, reflecting both endogenous phenolic and carbohydrate constituents and confirming that *P. pavonica* is a source of antioxidant phenolic monoterpenoids and derivatizable polyols (Makhlof *et al*., 2024).

Table 1. Volatile and semi-volatile components identified in *Padina pavonica* extract.

Gland Surg
VOL-11 NO 1 (2026)
ISSN:2227-684X | E-ISSN:2227-8575

RT (min)	Compound (as identified by library match)	Class / structural type	Area %	Molecular formula
24.13	Ethanol, 2-(9-octadecenyloxy)-, (Z)-	Ether-linked unsaturated fatty alcohol	3.16	$C_{20}H_{40}O_2$
26.66	Hexadecanoic acid, 2,3-dihydroxypropyl ester	Monoacylglycerol (palmitate derivative)	2.23	$C_{19}H_{38}O_4$
26.66	Oleic acid / 9-octadecenoic acid (Z)	Monounsaturated fatty acid	2.23	$C_{18}H_{34}O_2$
27.73	Arachidonic acid (5,8,11,14-eicosatetraenoic acid)	Polyunsaturated fatty acid (PUFA)	8.54	$C_{20}H_{32}O_2$
27.73	5,8,11,14-Eicosatetraenoic acid methyl/ethyl esters	PUFA methyl/ethyl esters	8.54	C_{21}–$C_{22}H_{34}$–$36O_2$
28.82	9-Octadecenoic acid (Z) (oleic acid)	Monounsaturated fatty acid	4.86	$C_{18}H_{34}O_2$
28.82	9-/10-Octadecenoic acid methyl esters	Monounsaturated FAMEs	4.86	$C_{19}H_{36}O_2$
29.13	1,2-15,16-Diepoxyhexadecane	Epoxy long-chain alkane	3.37	$C_{16}H_{30}O_2$
29.13	Cholestan-3-ol, 2-methylene-, (3α,5α)-	Sterol derivative	3.37	$C_{28}H_{48}O$
32.44	2-[4-Methyl-6-(2,6,6-trimethylcyclohex-1-enyl)hexa-1,3,5-trienyl]cyclohex-1-en-1-carboxaldehyde	Terpenoid-like aldehyde	0.95	$C_{23}H_{32}O$
32.44	Androstan-17-one, 3-ethyl-3-hydroxy-, (5α)-	Steroid	0.95	$C_{21}H_{34}O_2$
40.12	1-Heptatriacontanol	Long-chain fatty alcohol	2.11	$C_{37}H_{76}O$
40.12	Linolenic acid, 2-hydroxy-1-(hydroxymethyl)ethyl ester	Glycolipid / PUFA ester	2.11	$C_{21}H_{36}O_4$
41.08–43.00	9,12-Octadecadienoic acid (Z,Z)-, 2,3-bis[(trimethylsilyl)oxy]propyl ester	Silylated linoleic-acid ester	1.25–1.94	$C_{27}H_{54}O_4si_2$
41.08–43.00	Thymol / carvacrol TBDMS derivatives	Phenolic monoterpenoids (silylated)	1.25–1.60	$C_{16}H_{28}OSi$
41.08–43.00	Arabinitol pentaacetate	Polyol (sugar alcohol derivative)	1.25–1.94	$C_{15}H_{22}O_{10}$
41.92–	Methyl α-D-galactopyranoside	Silylated sugar	1.44–	$C_{17}H_{37}BO_6Si_2$

Gland Surg
VOL-11 NO 1 (2026)
ISSN:2227-684X | E-ISSN:2227-8575

RT (min)	Compound (as identified by library match)	Class / structural type	Area %	Molecular formula
43.00	trimethylsilyl boronates	derivatives	1.94	
44.73	Cholest-5-en-3-ol, 24-propylidene-, (3α)-	Cholesterol-type sterol	65.38	$C_{30}H_{50}O$
44.73	Stigmasta-5,24(28)-dien-3-ol, (3α,24Z)-	Phytosterol	65.38	$C_{29}H_{48}O$
44.73	Pregnane-type steroids (e.g., pregn-7-ene-3,20-dione; 3,17-dihydroxypregn-5-en-20-one)	Steroidal hormones/derivatives	65.38	$C_{21}H_{30}$–$32O_2$–3

This profile highlights that the volatile/semi-volatile fraction of *P. pavonica* is enriched in unsaturated fatty acids and esters, alongside a complex mixture of sterols, terpenoids, phenolic monoterpenes, and derivatized carbohydrates, which together may underpin the antioxidant, anti-inflammatory-, and lipid-modulating bioactivities ascribed to this brown alga.

3.2. Biological cytotoxicity activity

Treatment with *Padina pavonica* (PP) extract resulted in a dose-dependent reduction in cell viability in both A549 and MCF-7 cell lines. In A549 cells, the IC_{50} of PP extract was 60.73 µg/ml, while cisplatin (CP) exhibited a markedly lower IC_{50} of 1.32 µg/ml, indicating higher potency **(Fig. 2)**. In MCF-7 cells, PP extract showed an IC_{50} of 173.11 µg/ml, compared to 1.72 µg/ml for cisplatin **(Fig. 2)**.

Comparisons of cytotoxicity across concentrations (0.1–1000 µg/ml) revealed statistically significant reductions in viability at higher doses of both treatments. In A549 cells, PP extract showed significant cytotoxicity at 100 and 1000 µg/ml (**$p < 0.01$ and ***$p < 0.001$, respectively), while cisplatin was effective at much lower concentrations (**$p < 0.01$ at 10 µg/ml and ***$p < 0.001$ at 100 µg/ml). Similar trends were observed in MCF-7 cells, with PP extract showing significant effects only at 1000 µg/ml (***$p < 0.001$), whereas cisplatin induced strong cytotoxicity starting from 10 µg/ml (**$p < 0.01$) (Fig. 1C). These findings confirm the cytotoxic potential of *Padina pavonica* extract, albeit at higher concentrations than cisplatin, and support its role as a candidate anticancer agent **(Fig. 2)**.

The differential IC_{50} values observed between the PP extract and cisplatin reflect distinct modes of action. Cisplatin, a DNA-damaging agent, exerts cytotoxicity through direct genotoxic stress, while PP extract likely engages broader cellular pathways, including redox modulation and signaling interference. The higher IC_{50} of the PP extract may indicate a multi-targeted but less aggressive mechanism, aligning with the hypothesis that marine natural products restore cellular balance rather than induce acute damage.

The cytotoxicity induced by *Padina pavonica* may be viewed not as a blunt force intervention, but as a gradual dismantling of the cancer cell's survival architecture. The ability of the extract to reduce viability at high doses suggests a threshold-dependent activation of stress responses, potentially involving apoptosis and cell cycle arrest, which will be explored in subsequent assays.

Gland Surg
VOL-11 NO 1 (2026)
ISSN:2227-684X | E-ISSN:2227-8575

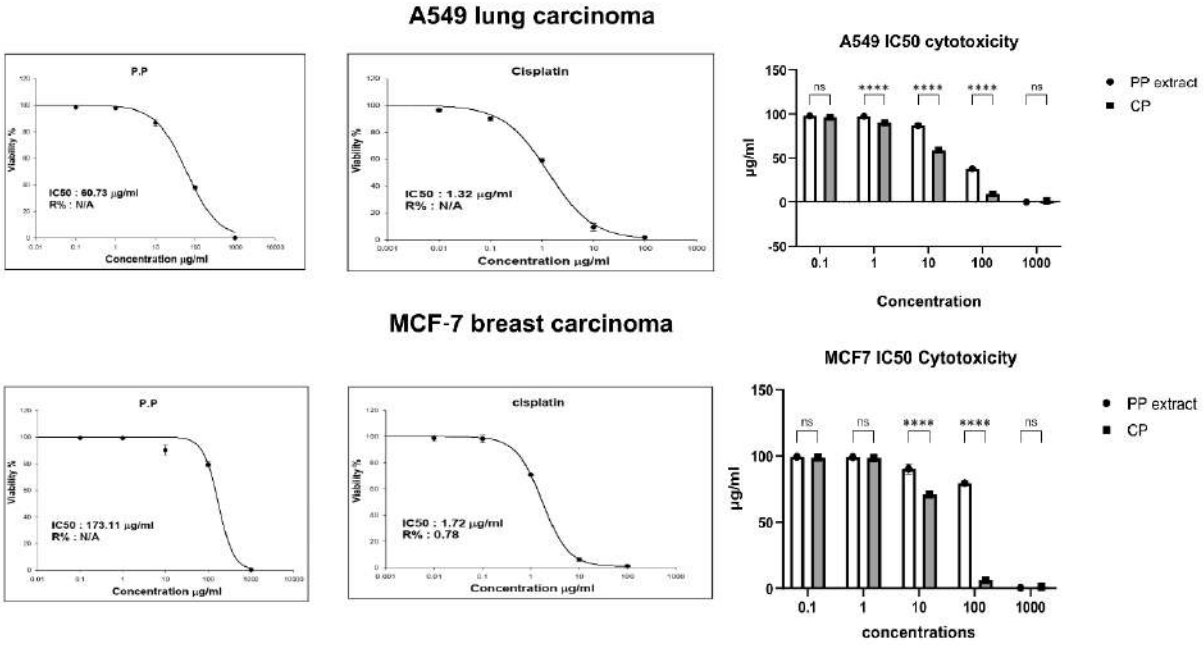

Figure 2. *Padina pavonica* extract reduces cell viability in A549 and MCF-7 carcinoma cells in a dose-dependent manner.

Cytotoxic effects of *Padina pavonica* (PP) extract and cisplatin (CP) on A549 lung carcinoma (top row) and MCF-7 breast carcinoma (bottom row) cells after 48-hour treatment. (A, D) Dose-response curves showing the percentage of cell viability across increasing concentrations of PP extract. IC50 values were 60.73 µg/mL for A549 and 173.11 µg/mL for MCF-7. (B, E) Dose-response curves for CP treatment, with IC50 values of 1.32 µg/mL (A549) and 1.72 µg/mL (MCF-7), confirming higher potency. (C, F) Bar graphs comparing cytotoxicity at selected concentrations (0.1–1000 µg/mL) for PP and CP. Statistical significance was assessed using one-way ANOVA; *p < 0.05, **p < 0.01, ***p < 0.001, ****p < 0.0001, ns = not significant. Data represent the mean ± SD from three independent experiments.

3.3. Morphological Assessment

Microscopic examination revealed dose-dependent morphological alterations in both A549 and MCF-7 cells following treatment with *the Padina pavonica* extract. In A549 cells, increasing concentrations (10, 100, and 1000 µg/ml) led to progressive reductions in cell density, loss of adherence, and rounding of cells, with the 1000 µg/ml group showing marked cytoplasmic shrinkage and detachment from the substrate **(Fig. 3)**. These features are consistent with cytotoxic stress and apoptotic morphology.

Moreover, MCF-7 cells exhibited similar trends, although they were less pronounced. At 1000 µg/ml, cells showed reduced confluence, rounding, and partial detachment, suggesting sublethal stress or early apoptotic changes **(Fig. 3)**. Compared to A549 cells, MCF-7 cells appeared more resistant morphologically, aligning with the higher IC_{50} observed in viability assays. These visual findings support the cytotoxic effect of *Padina pavonica* extract and reinforce its dose-dependent impact on cellular integrity.

The observed morphological changes reflect the ability of the extract to disrupt cellular architecture, a hallmark of apoptosis and cytotoxicity. In A549 cells, the pronounced detachment and

shrinkage at 1000 µg/ml mirror classical apoptotic features, suggesting activation of intrinsic death pathways. In MCF-7 cells, the subtler morphological response may indicate delayed or partial engagement of apoptotic mechanisms, consistent with their known resistance to caspase-dependent apoptosis due to low caspase-3 expression. This differential response between cell lines highlights the importance of cell-specific context in evaluating the efficacy of natural products.

In contrast to cisplatin, which provokes an abrupt and forceful collapse of cells through both necrotic and apoptotic mechanisms, *Padina pavonica* seems to initiate a slower and more progressive sequence of morphological alterations. This gradual transition underscores its functional identity as a regulator of cellular equilibrium, positioning it as a modulator of survival pathways rather than as a conventional, aggressively acting cytotoxic compound.

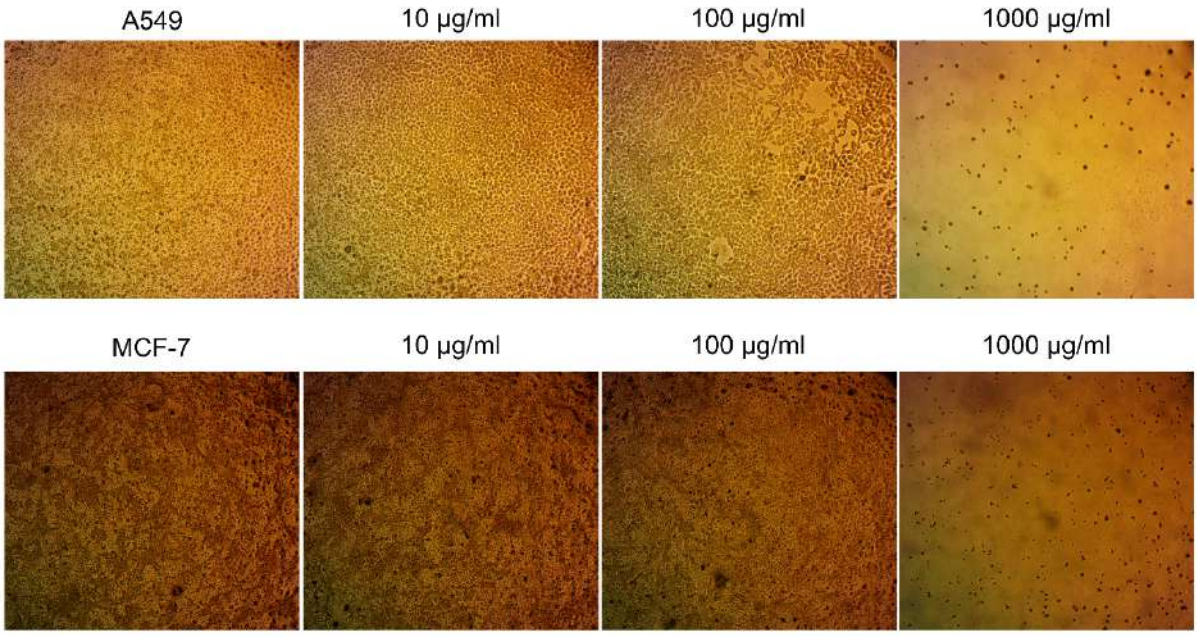

Figure 3. *Padina pavonica methanolic* extract induces concentration-dependent morphological alterations in A549 and MCF-7 carcinoma cells.
Representative phase-contrast micrographs of A549 lung carcinoma (top row) and MCF-7 breast carcinoma (bottom row) cells after 48-hour treatment with Padina pavonica (PP) extract at 10, 100, and 1000 µg/mL. The untreated control cells (far left) maintained their normal morphology, adherence, and confluence. PP-treated cells exhibited progressive morphological changes with increasing concentrations, including cell shrinkage, rounding, membrane blebbing, detachment, and reduced cell density, which are hallmarks of cytotoxic and apoptotic responses. Scale bar = 10×.

3.4. Apoptosis Induction

Flow cytometry analysis revealed a significant increase in apoptotic cell populations following treatment with *Padina pavonica* extract and cisplatin. In untreated A549 cells (control), the majority of cells remained viable **(Q2-3:96.53%)**, with minimal early **(Q2-4:1.22%)** or late apoptosis **(Q2-2:1.65%) (Fig. 4A)**. Treatment with PP extract led to a marked increase in late apoptotic cells **(Q2-2:12.48%)** and early apoptotic cells **(Q2-4:0.22%)**, with a corresponding decrease in viable cells **(Q2-3:80.80%) (Fig. 4B)**. Cisplatin treatment induced both early **(Q2-4:9.80%)** and late apoptosis **(Q2-2:9.74%)**, reducing cell viability to 71.17% **(Fig. 4C)**.

Gland Surg
VOL-11 NO 1 (2026)
ISSN:2227-684X | E-ISSN:2227-8575

Quantitative analysis **(Fig. 4D)** confirmed that both PP extract and CP significantly increased total apoptotic cell percentages compared to the control. PP extract showed a significant increase in late apoptosis (**$p < 0.01$), while cisplatin induced a broader apoptotic response across the early and late phases (***$p < 0.001$). Viable cell percentages were significantly reduced in both treatments (****$p < 0.0001$), confirming the cytotoxic engagement of apoptotic pathways. These results demonstrate that *Padina pavonica* extract activates apoptosis in A549 cells, supporting its role as a mechanistic anticancer agent.

The induction of apoptosis by *Padina pavonica* extract reflects its ability to engage intrinsic death pathways, a hallmark of effective anticancer agents. The predominance of late apoptosis suggests mitochondrial involvement, potentially through modulation of Bax/Bcl-2 ratios, which will be explored in subsequent assays. Compared to cisplatin, which triggers both early and late apoptosis, PP extract appears to favor a delayed apoptotic onset, possibly due to its gradual disruption of survival signaling. Notably, the apoptotic profile of the PP extract resembled that of fucoidan-rich fractions from *Fucus vesiculosus*, which also favored late apoptosis and PI3K/AKT pathway suppression.

Conceptually, apoptosis here is not merely a cell death endpoint but a restoration of cellular equilibrium -a reassertion of programmed fate in cells that have escaped regulatory control. *Padina pavonica* extract, by nudging cells back toward this fate, exemplifies the therapeutic principle of rebalancing rather than obliterating, distinguishing it from the more aggressive cytotoxicity of cisplatin.

In contrast, flow cytometry revealed a significant increase in apoptotic cell populations in MCF-7 cells following treatment with *Padina pavonica* extract and cisplatin. In the untreated controls, the majority of cells remained viable **(Q2-3:98.30%)**, with minimal early **(Q2-4:0.28%)** or late apoptosis **(Q2-2:1.02%) (Fig. 5A)**. Treatment with PP extract led to a substantial increase in late apoptotic cells **(Q2-2:14.75%)** and necrotic cells **(Q2-1:17.48%)**, reducing viability to 67.69% **(Fig. 5B)**. Cisplatin induced early apoptosis **(Q2-4:17.07%)** and moderate late apoptosis **(Q2-2:6.03%)**, with viability reduced to 70.47% **(Fig. 5C)**.

Quantitative analysis **(Fig. 5D)** confirmed that PP extract significantly increased late apoptosis and necrosis compared to the control (***$p < 0.001$, and ****$p < 0.0001$, respectively), while cisplatin primarily elevated early apoptosis (***$p < 0.001$). Viable cell percentages were significantly reduced in both treatments (****$p < 0.0001$), confirming the activation of cell death pathways. These findings demonstrate that *Padina pavonica* extract induces apoptosis and necrosis in MCF-7 cells, supporting its cytotoxic potential and suggesting a distinct mechanistic profile compared to cisplatin.

The apoptotic response in MCF-7 cells revealed a nuanced mechanism of action for *Padina pavonica* extract. The dominance of late apoptosis and necrosis suggests mitochondrial involvement and possible membrane destabilization, in contrast to cisplatin's early apoptotic induction via DNA damage and ROS generation. This divergence may reflect differences in intracellular uptake, caspase activation, or redox modulation.

MCF-7 cells are known to be caspase-3 deficient, often exhibiting resistance to classical apoptosis (Yang *et al*., 2001). The ability of PP extract to bypass this resistance and induce late apoptosis and necrosis suggests engagement of alternative death pathways, such as caspase-independent apoptosis or autophagy-associated cell death.

The apoptotic shift induced by *Padina pavonica* represents a reassertion of programmed cellular fate

Gland Surg
VOL-11 NO 1 (2026)
ISSN:2227-684X | E-ISSN:2227-8575

in a resistant phenotype. Unlike cisplatin's rapid apoptotic onset, PP extract appears to gradually destabilize survival architecture, allowing for broader engagement of death pathways. This supports the hypothesis that marine natural products act as multi-targeted modulators, restoring cellular balance through layered biochemical interventions.

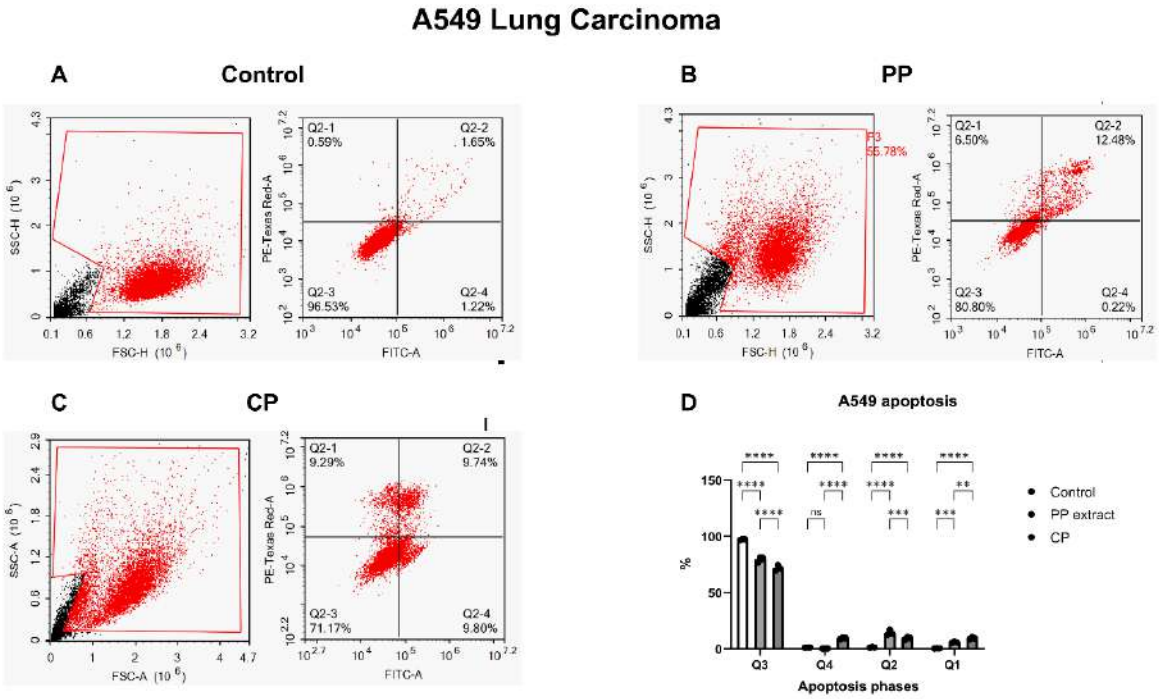

Figure 4. ***Padina pavonica*** **extract induces apoptosis in A549 lung carcinoma cells.**
Flow cytometric analysis of apoptosis in A549 cells treated with *Padina pavonica* (PP) extract or cisplatin (CP) for 48 h using annexin V-FITC/PI staining. (A) Untreated control cells displayed predominantly viable populations (Q3) with minimal apoptotic or necrotic activity. (B) PP extract treatment increased early apoptotic (Q2) and late apoptotic/necrotic (Q1) populations, indicating the activation of intrinsic apoptotic pathways. (C) CP treatment markedly enhanced apoptosis, with a higher proportion of Annexin V-positive cells across both the early and late phases. (D) Quantitative analysis of apoptotic and necrotic cell populations across treatments. Data are presented as the mean ± SD from three independent experiments. Significance levels: *p < 0.05, **p < 0.01, ***p < 0.001, ****p < 0.0001, ns = not significant.

Gland Surg
VOL-11 NO 1 (2026)
ISSN:2227-684X | E-ISSN:2227-8575

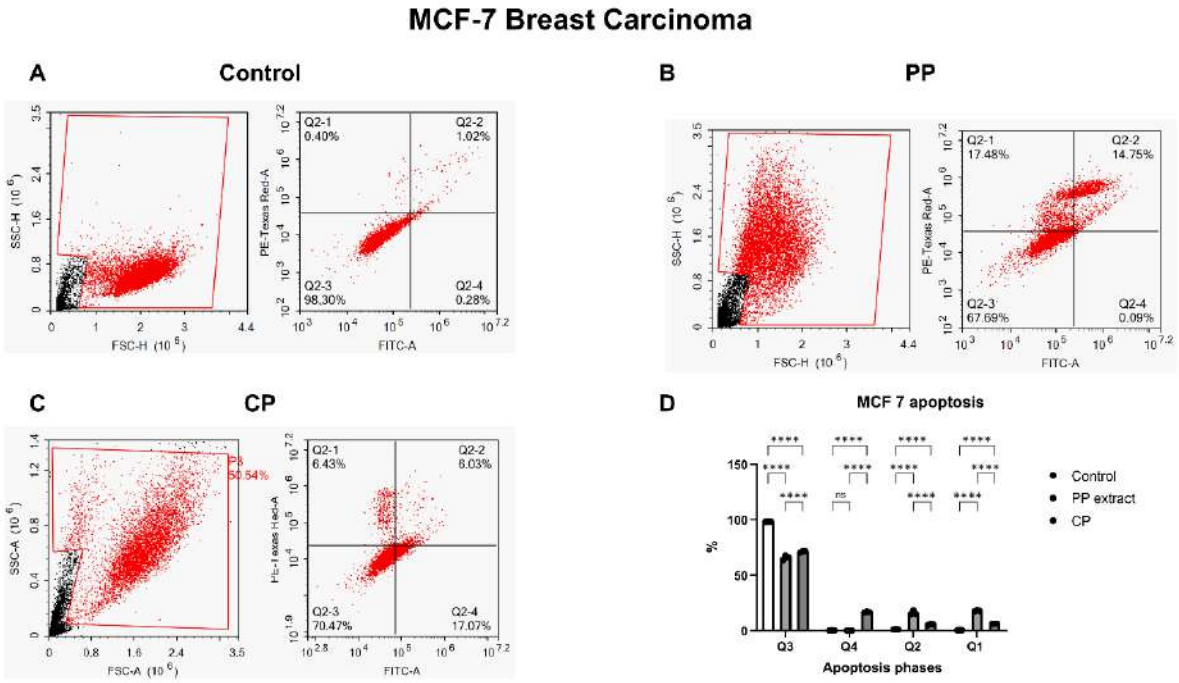

Figure 5. ***Padina pavonica*** **extract promotes apoptosis in MCF-7 breast carcinoma cells.** Flow cytometric analysis of apoptosis in MCF-7 cells treated with *Padina pavonica* (PP) extract or cisplatin (CP) for 48 h using Annexin V-FITC/PI staining. (A) Untreated control cells displayed predominantly viable populations (Q3) with minimal apoptotic or necrotic activity. (B) PP extract treatment increased both late apoptotic/necrotic (Q1) and early apoptotic (Q2) populations, indicating activation of apoptosis despite caspase-3 deficiency in MCF-7 cells. (C) CP treatment markedly enhanced apoptosis, with elevated annexin V-positive cells across all apoptotic phases. (D) Quantitative analysis of apoptotic and necrotic cell populations across treatments. Data are presented as the mean ± SD from three independent experiments. Significance levels: *p < 0.05, **p < 0.01, ***p < 0.001, ****p < 0.0001, ns = not significant.

3.5. Cell Cycle Modulation

Flow cytometric analysis revealed significant alterations in cell cycle distribution following treatment with *Padina pavonica* extract and cisplatin. In untreated A549 cells, the majority of cells were in the G1 phase, with balanced proportions in the S and G2 phases, and a minimal sub-G1 population **(Fig. 6A)**. Treatment with the PP extract led to a marked accumulation of cells in the G1 phase and a reduction in the S phase, indicating G1 arrest **(Fig. 6B)**. Cisplatin treatment resulted in a pronounced increase in the sub-G1 population, consistent with apoptotic DNA fragmentation, and a reduction in G2 phase cells **(Fig. 6C)**.

Quantitative analysis **(Fig. 6D)** showed that PP extract significantly increased the G1 phase percentage (**p < 0.01) and decreased the S phase (*p < 0.05), whereas cisplatin significantly elevated the sub-G1 population (****p < 0.0001) and reduced the G2 phase (**p < 0.01). These findings suggest that *Padina pavonica* extract induces cell cycle arrest at G1, whereas cisplatin promotes apoptotic collapse reflected in sub-G1 accumulation.

The G1 arrest induced by *Padina pavonica* extract in A549 cells indicates disruption of the cell's proliferative momentum, a critical anticancer mechanism. G1 phase accumulation suggests

interference with cyclin D/CDK4/6 activity or upstream signaling, such as PI3K/AKT, which will be examined in subsequent assays. In contrast, cisplatin elevation of sub-G1 reflects DNA fragmentation and apoptotic progression, consistent with its genotoxic profile.

Cell cycle arrest represents a pause in the narrative of unchecked proliferation - a moment where the cell is forced to reassess its trajectory. *Padina pavonica* extract, by inducing G1 arrest, acts as a regulatory checkpoint, restoring control over cell fate. This contrasts with cisplatin's more abrupt intervention, reinforcing the idea that natural products may offer a gentler but strategic disruption of cancer cell dynamics.

Flow cytometric analysis revealed distinct changes in cell cycle distribution in MCF-7 cells following treatment with *Padina pavonica* extract and cisplatin. In untreated controls, the majority of cells were in the G1 phase, with balanced proportions in the S and G2 phases, and a minimal sub-G1 population **(Fig. 7A)**. Treatment with PP extract led to a significant increase in the sub-G1 population (****$p < 0.0001$), indicative of apoptotic DNA fragmentation, and a reduction in the G2 phase (**$p < 0.01$) **(Fig. 7B)**. Similarly, cisplatin treatment similarly elevated sub-G1 levels (***$p < 0.001$) and reduced G2 phase (**$p < 0.01$), with no significant change in G1 or S phases **(Fig. 7C)**.

Quantitative analysis **(Fig. 7D)** confirmed that both treatments disrupted normal cell cycle progression, with the PP extract showing a stronger apoptotic signature via sub-G1 accumulation. These findings suggest that *Padina pavonica* extract induces cell death in MCF-7 cells through cell cycle disruption, complementing its apoptotic effects.

The increase in the sub-G1 population following *Padina pavonica* treatment reflects DNA fragmentation and apoptotic progression, consistent with prior flow cytometry results. The reduction in the G2 phase suggests interference with mitotic entry, possibly through checkpoint inhibition or DNA damage response activation. Compared to cisplatin, which showed a similar but less pronounced effect, PP extract appears to engage cell cycle disruption as a secondary mechanism of cytotoxicity.

The ability of PP extract to bypass G1/S control and directly elevate sub-G1 levels suggests a caspase-independent apoptotic pathway, which is particularly relevant given MCF-7's caspase-3 deficiency. The shift toward sub-G1 reflects a collapse of proliferative identity, a point where the cell no longer maintains genomic integrity or division potential. *Padina pavonica* extract, by inducing this collapse, acts as a disruptor of the cancer cell's temporal momentum, halting its forward trajectory and restoring control through programmed death. This complements its apoptotic and morphological effects, reinforcing its role as a multi-targeted anticancer agent.

Gland Surg
VOL-11 NO 1 (2026)
ISSN:2227-684X | E-ISSN:2227-8575

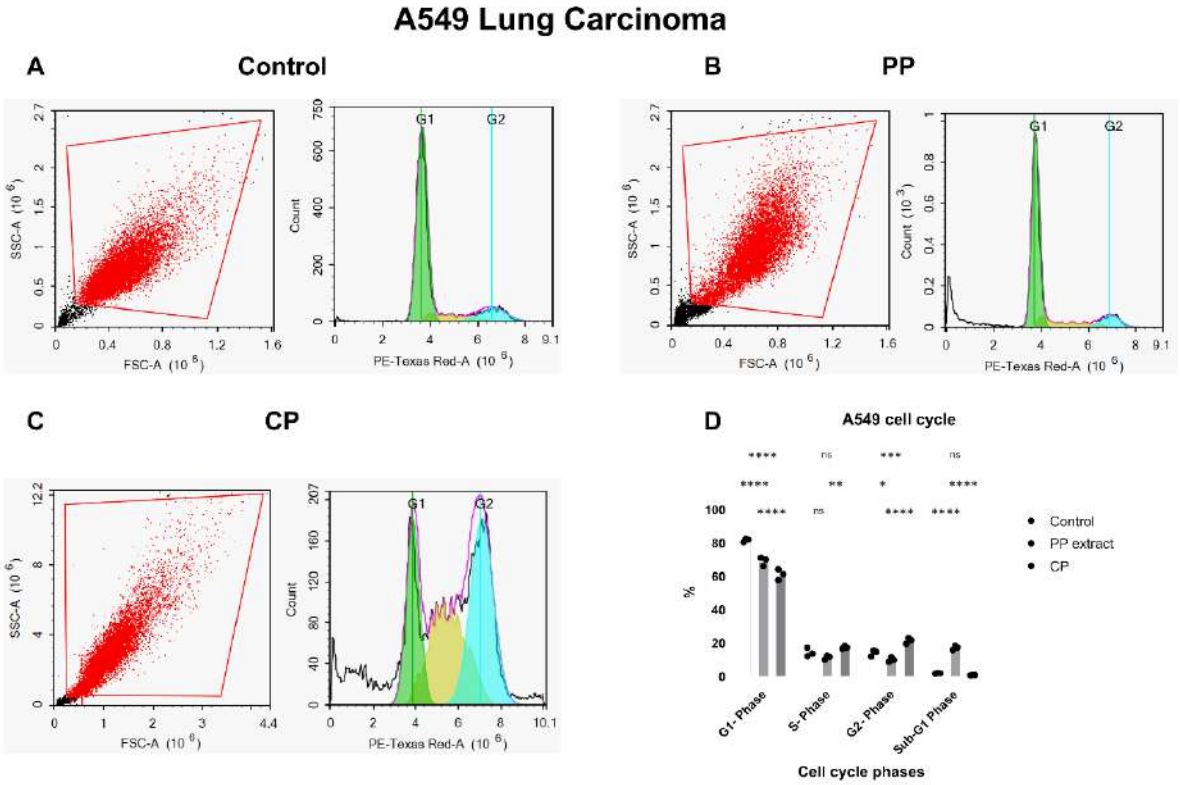

Figure 6. *Padina pavonica* extract alters cell cycle distribution in A549 lung carcinoma cells. Flow cytometric analysis of cell cycle phases in A549 cells treated with *Padina pavonica* (PP) extract or cisplatin (CP) for 48 h using PI staining. (A) Untreated control cells displayed a typical distribution across the G1, S, and G2/M phases. (B) PP extract treatment induced accumulation in the G1 phase and a modest increase in the sub-G1 population, indicating cell cycle arrest and apoptotic entry. (C) CP treatment caused pronounced G2/M arrest and elevated the sub-G1 fraction, consistent with DNA fragmentation and apoptosis. (D) Quantitative comparison of cell cycle phase distribution across treatments. Data are presented as the mean ± SD from three independent experiments. Significance levels: *p < 0.05, **p < 0.01, ***p < 0.001, ****p < 0.0001, ns = not significant.

Gland Surg
VOL-11 NO 1 (2026)
ISSN:2227-684X | E-ISSN:2227-8575

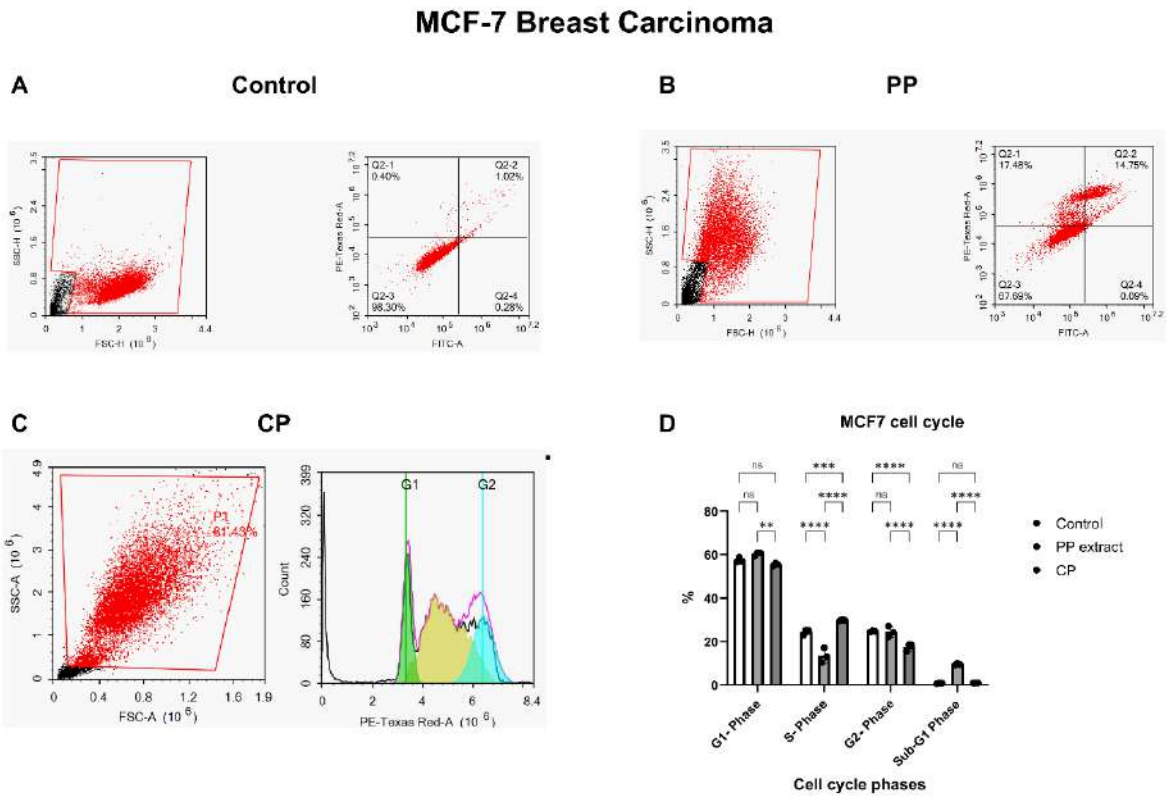

Figure 7. *Padina pavonica* extract modulates cell cycle progression in MCF-7 breast carcinoma cells.

Flow cytometric analysis of cell cycle distribution in MCF-7 cells treated with *Padina pavonica* (PP) extract or cisplatin (CP) for 48 h using PI staining. (A) Untreated control cells showed a typical distribution across the G1, S, and G2/M phases. (B) PP extract treatment induced accumulation in the G1 phase and a modest increase in the sub-G1 population, suggesting cell cycle arrest and apoptotic entry. (C) CP treatment caused pronounced G2/M arrest and elevated the sub-G1 fraction, consistent with DNA fragmentation and apoptosis. (D) Quantitative comparison of cell cycle phase distribution across treatments. Data are presented as the mean ± SD from three independent experiments. Significance levels: *p < 0.05, **p < 0.01, ***p < 0.001, ****p < 0.0001, ns = not significant.

3.6. Glutathione (GSH) and Total Antioxidant Capacity

To better understand how *Padina pavonica* (PP) extract affects oxidative stress regulation, researchers assessed intracellular glutathione (GSH) levels and overall antioxidant capacity in A549 and MCF-7 cells. In A549 cells, the untreated control group showed a baseline GSH level of 0.80 mg/dL and a total antioxidant capacity of 0.47 mg/dL. Upon treatment with PP extract, there was a significant drop in GSH to 0.37 mg/dL, along with a slight decrease in antioxidant capacity to 0.40 mg/dL. This simultaneous reduction suggests that the PP extract weakens both specific thiol-based defenses and the general antioxidant system. The reduction in GSH, a key regulator of redox balance, implies that PP extract induces oxidative stress, making A549 cells more susceptible to apoptosis. The accompanying decrease in total antioxidant capacity supports this view, emphasizing oxidative imbalance as a factor contributing to the observed increase in Bax, decrease in Bcl-2, and inhibition of the PI3K/AKT pathway.

Gland Surg
VOL-11 NO 1 (2026)
ISSN:2227-684X | E-ISSN:2227-8575

In MCF-7 cells, the control group exhibited a baseline GSH level of 0.47 mg/dL and an antioxidant capacity of 0.37 mg/dL. After treatment with PP, GSH levels were undetectable, indicating either complete depletion or measurement interference due to severe oxidative stress. The antioxidant capacity also significantly decreased to 0.13 mg/dL. This reduction in both GSH and total antioxidant defenses suggests that PP extract imposes significant oxidative stress on MCF-7 cells. This depletion likely contributes to the induction of late apoptosis and necrosis observed by flow cytometry, aligning with the caspase-3 deficiency in this cell line, which often requires alternative cell death pathways.

These results demonstrate that *Padina pavonica* extract significantly undermines redox balance in both A549 and MCF-7 cells, although with differing intensities. In A549 cells, oxidative stress is evident but partial, complementing apoptotic signaling. In MCF-7 cells, antioxidant defenses collapse almost entirely, forcing cells into death pathways despite their resistance to classical apoptosis. The combined depletion of GSH and total antioxidant capacity underscores oxidative stress as a central mechanism of PP-induced cytotoxicity, reinforcing its role as a multitargeted modulator of cancer cell survival.

3.7. RT-qPCR *Gene Expression*

RT-qPCR analysis revealed differential modulation of apoptosis and survival pathway genes in A549 and MCF-7 cells following treatment with Padina pavonica extract. In A549 cells, PP treatment significantly upregulated Bax (****$p < 0.0001$) and downregulated Bcl-2 (*$p < 0.05$), indicating the activation of intrinsic apoptotic signaling **(Fig. 8)**. Additionally, PI3K (**$p < 0.01$) and AKT1 (*$p < 0.05$) expression was significantly reduced, suggesting suppression of the PI3K/AKT survival pathway.

In MCF-7 cells, the expression of Bax did not reveal a significant change, whereas that of Bcl-2 was notably reduced (*$p < 0.05$), indicating a partial activation of apoptotic signaling (Fig. 8). Notably, PI3K levels increased (*$p < 0.05$), while AKT1 levels decreased (*$p < 0.05$), indicating a complex alteration in survival signaling that differs from the A549 profile. These findings demonstrate that Padina pavonica extract influences key genes involved in apoptosis and survival, with patterns specific to each cell line, reflecting varying sensitivity and pathway activation.

The increase in Bax and decrease in Bcl-2 levels in A549 cells enhanced the pro-apoptotic impact of the extract, aligning with previous flow cytometry and cell cycle findings. The simultaneous inhibition of PI3K and AKT1 indicates a coordinated blockade of survival pathways, supporting the theory that Padina pavonica undermines cancer cell resilience by modulating multiple pathways. In MCF-7 cells, the absence of Bax induction and the increase in PI3K may indicate compensatory survival mechanisms, possibly due to the cell line's lack of caspase-3 and altered apoptotic processes. However, the reduction in AKT1 suggests partial inhibition of downstream survival factors, implying that *Padina pavonica* has a modulatory rather than an all-or-nothing effect on resistant phenotypes. The distinct gene expression patterns between A549 and MCF-7 cells highlight the significance of cellular context in determining therapeutic outcomes. These changes in gene expression represent a reconfiguration of cellular decision-making, adjusting the balance between survival and death signals. *Padina pavonica* extract functions not as a single-target agent but as a systemic modulator, steering cells toward apoptosis by shifting the molecular equilibrium. This complex interaction supports its potential as a biologically intelligent anticancer candidate capable of adapting its effects across different cellular environments.

Gland Surg
VOL-11 NO 1 (2026)
ISSN:2227-684X | E-ISSN:2227-8575

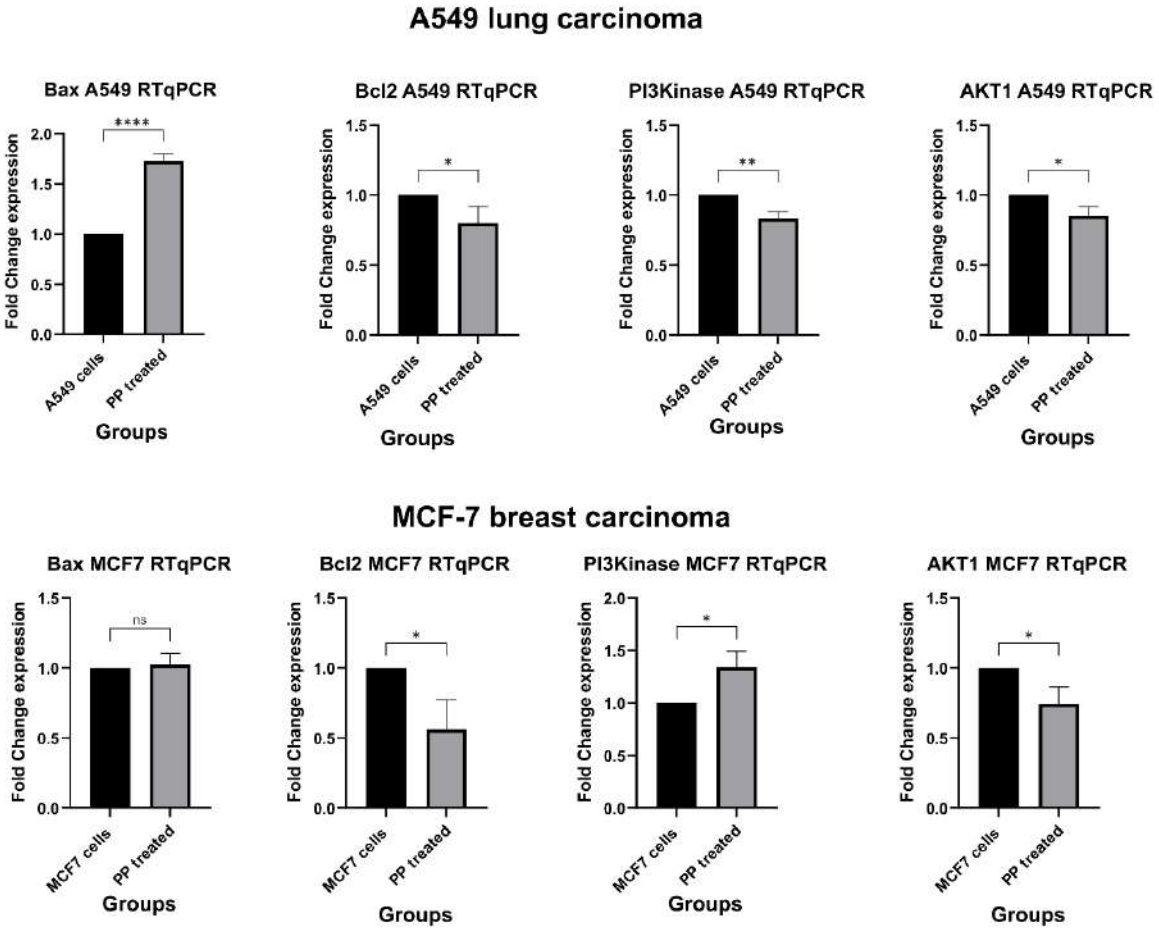

Figure 8. Padina pavonica extract modulates expression of apoptosis and survival-related genes in A549 and MCF-7 carcinoma cells.

Quantitative RT-qPCR analysis of Bax, Bcl-2, PI3K, and AKT1 gene expression in A549 lung carcinoma (top row) and MCF-7 breast carcinoma (bottom row) cells following treatment with Padina pavonica (PP) extract. In A549 cells, PP treatment significantly upregulated pro-apoptotic Bax (****$p < 0.0001$) and downregulated anti-apoptotic Bcl-2 ($p < 0.05$), PI3K ($p < 0.01$), and AKT1 ($p < 0.05$), indicating suppression of survival signaling. In MCF-7 cells, PP treatment reduced Bcl-2 ($p < 0.05$) and AKT1 ($p < 0.05$) expression, while Bax expression remained unchanged (ns), and PI3K was modestly upregulated (*$p < 0.05$), reflecting cell line-specific transcriptional responses. Data are presented as fold change ± SD from three independent experiments. Significance levels: *$p < 0.05$, **$p < 0.01$, ***$p < 0.001$, ****$p < 0.0001$, ns = not significant.

3.8. Protein Expression

Western blot analysis was performed to evaluate the impact of *Padina pavonica* (PP) extract on key apoptotic and survival signaling proteins in A549 and MCF-7 cells. The expression levels of Bax, Bcl-2, PI3K-p85, and phosphorylated AKT (p-AKT) were assessed, with β-actin serving as the internal loading control **(Fig. 9)**. In MCF-7 cells, treatment with PP extract resulted in a noticeable shift in the expression profile of apoptosis-related and survival proteins. Quantitative densitometric analysis revealed significant upregulation of Bax (**$p < 0.01$), indicating the activation of

Gland Surg
VOL-11 NO 1 (2026)
ISSN:2227-684X | E-ISSN:2227-8575

pro-apoptotic signaling. Concurrently, Bcl-2 expression was significantly downregulated (*$p < 0.05$), suggesting the suppression of anti-apoptotic defense mechanisms **(Fig. 9I)**.

Regarding survival signaling, the PP extract led to a significant reduction in PI3K-p85 levels (**$p < 0.01$), accompanied by a highly significant decrease in p-AKT expression (****$p < 0.0001$). These changes reflect the inhibition of the PI3K/AKT pathway, which is commonly associated with cell survival, proliferation, and resistance to apoptosis. The combined modulation of these proteins suggests that the PP extract disrupts the balance between pro- and anti-apoptotic signals, favoring apoptotic progression even in the caspase-3-deficient MCF-7 phenotype **(Fig. 9II)**.

In A549 cells, PP extract induced a robust pro-apoptotic response. Bax expression was significantly elevated (***$p < 0.001$), while Bcl-2 levels were markedly suppressed (****$p < 0.0001$), indicating strong activation of the intrinsic apoptotic pathway. The extract also exerted a pronounced inhibitory effect on survival signaling. PI3K-p85 expression was significantly reduced (*$p < 0.05$), and p-AKT levels were downregulated (**$p < 0.01$), confirming the suppression of the PI3K/AKT axis. These changes align with earlier gene expression data and reinforce the notion that PP extract promotes apoptosis through coordinated downregulation of survival pathways and upregulation of death signals **(Fig. 8)**.

The differential protein expression profiles between A549 and MCF-7 cells underscored the cell-specific responsiveness to the PP extract. In A549 cells, the extract triggered a classical apoptotic cascade with strong Bax induction and PI3K/AKT inhibition. In MCF-7 cells, despite the absence of caspase-3, PP extract successfully modulated upstream regulators, suggesting engagement of alternative apoptotic mechanisms or caspase-independent pathways.

These protein-level findings complement the flow cytometry and gene expression data, providing molecular confirmation that *Padina pavonica* extract acts as a multi-targeted modulator of cell fate. By simultaneously activating pro-apoptotic signals and suppressing survival pathways, the extract orchestrated a shift toward programmed cell death, reinforcing its therapeutic potential in both responsive and resistant cancer phenotypes.

Gland Surg
VOL-11 NO 1 (2026)
ISSN:2227-684X | E-ISSN:2227-8575

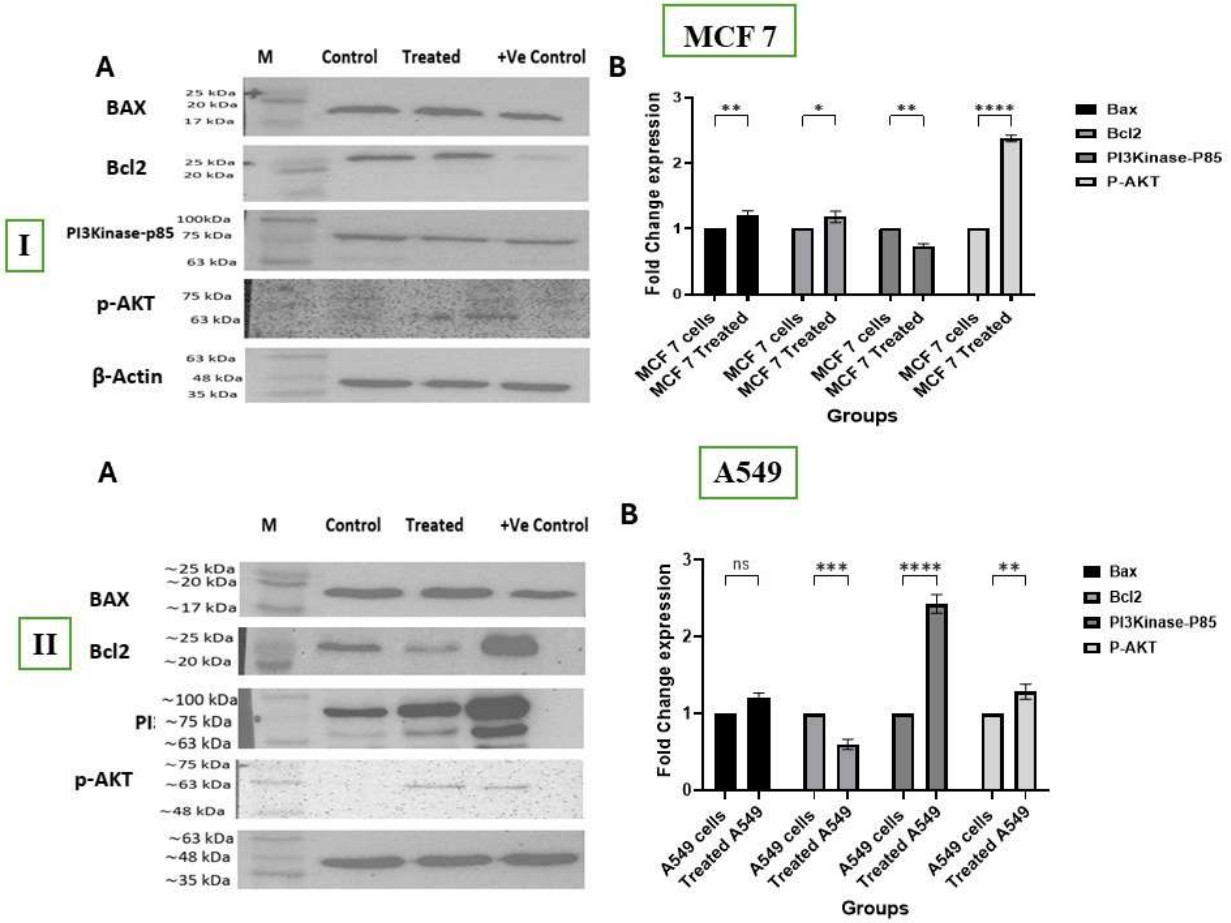

Figure 9. Effect of *Padina pavonica* extract on protein expression in A549 and MCF-7 cells.

(I) Protein expression analysis in MCF-7 cells. (A) Representative Western blot images showing expression levels of pro-apoptotic Bax, anti-apoptotic Bcl-2, PI3K-p85, and phosphorylated AKT (p-AKT) following treatment with *Padina pavonica* extract (Treated) compared to untreated controls (Control) and cisplatin-treated cells (+Ve Control). β-actin was used as a loading control. (B) Quantitative densitometric analysis of the fold change in protein expression relative to the control. PP extract significantly upregulated Bax ($p < 0.01$), downregulated Bcl-2 (*$p < 0.05$), and suppressed PI3K-p85 (**$p < 0.01$) and p-AKT (****$p < 0.0001$).

(II) Protein expression analysis in A549 cells. (A) Western blot images showing the expression of Bax, Bcl-2, PI3K-p85, and p-AKT in the control, PP-treated, and cisplatin-treated groups. β-actin served as a loading control. (B) Bar graph showing the fold change in protein levels. PP extract significantly increased Bax expression (***$p < 0.001$), reduced Bcl-2 (****$p < 0.0001$), and downregulated PI3K-p85 (*$p < 0.05$) and p-AKT (**$p < 0.01$). These data support the activation of intrinsic apoptotic signaling and suppression of survival pathways in both cell lines.

4. Discussion

Breast cancer and lung carcinoma are the two most prevalent and lethal malignancies worldwide. Breast cancer, driven by hormonal and genetic factors, is characterized by uncontrolled cell growth and metastasis. It is the most common cancer among women and its risk factors include age, family history, and lifestyle choices (Giaquinto et al., 2022). Lung carcinoma, associated with smoking and environmental exposure, is the leading cause of cancer-related deaths globally. It

includes various subtypes, with non-small cell lung cancer (NSCLC) being the most common and characterized by aggressive early metastasis (de Martel et al., 2020). Both cancers have seen advancements in targeted therapies and immunotherapy, improving survival rates, yet significant public health concerns remain that require ongoing research.

This study demonstrates that *Padina pavonica* extract exhibits anticancer properties in A549 lung carcinoma and MCF-7 breast carcinoma cells by inducing cytotoxicity, promoting apoptosis, disrupting the cell cycle, and modulating survival signaling. Although cisplatin showed greater potency, it also resulted in increased genotoxicity. These findings suggest that *Padina pavonica* acts as a modulator of cellular fate, restoring balance by dismantling survival pathways and reactivating cell death mechanisms.

Furthermore, cytotoxicity assays demonstrated dose-dependent reductions in cell viability, with IC50 values of 60.73 µg/ml in A549 cells and 173.11 µg/ml in MCF-7 cells compared to 1.32 µg/ml and 1.72 µg/ml for cisplatin, respectively. Although PP exhibited lower potency, its activity aligns with existing reports of brown algal metabolites exerting anticancer effects at elevated concentrations. For instance, fucoidan derived from Fucus vesiculosus has been shown to inhibit the migration and invasion of lung cancer cells through the suppression of the PI3K–AKT–mTOR pathway, whereas phlorotannins from the same species have been observed to activate apoptotic signaling in gastrointestinal tumor lines (Lee *et al*., 2012; Jin *et al*., 2022). Similarly, polysaccharides from *Sargassum muticum* showed antiproliferative activity and checkpoint effects in breast and lung cancer models (Namvar *et al*., 2013; Wang *et al*., 2025). These parallels reinforce the role of brown algae as modulators of cancer cell viability through multi-targeted mechanisms.

The results of our study indicate that *Padina pavonica* extract significantly reduces intracellular glutathione (GSH) levels and decreases total antioxidant capacity, particularly in MCF-7 cells. These findings align with those of previous studies that underscore the oxidative stress-inducing potential of brown algae. Makhlof *et al*. (2024) demonstrated that *P. pavonica* biomass extract exhibited strong antioxidant and antitumor activities, suggesting that modulation of redox balance is a key mechanism underlying its cytotoxicity. Similarly, sulfated polysaccharides isolated from *P. pavonica* were shown to exert antioxidant and anticancer effects by impairing cellular defenses against reactive oxygen species (ROS) (Palpperumal *et al*., 2024). These parallels reinforce the role of oxidative stress disruption as a complementary pathway through which *P. pavonica* enhances cancer cell susceptibility to apoptosis.

Apoptosis analysis confirmed that PP extract induces late apoptosis in A549 cells and a combination of late apoptosis and necrosis in MCF-7 cells, whereas cisplatin triggers both early and late apoptosis. This pattern suggests mitochondrial involvement in A549 and caspase-independent pathways in MCF-7, consistent with the latter's known caspase-3 deficiency. Comparable findings have been reported for selenium-enriched polysaccharide–protein complexes from *Ulva fasciata*, which induce mitochondria-mediated apoptosis in A549 cells (Górska *et al*., 2021). In MCF-7 cells, fucoidan from *Turbinaria conoides* demonstrated dose-dependent cytotoxicity despite partial resistance, mirroring our observation of PP's ability to bypass apoptotic resistance through alternative pathways (Santhanam *et al*., 2013).

Cell cycle analysis further demonstrated that PP induced G1 arrest in A549 cells and increased sub-G1 populations in MCF-7 cells, indicating apoptotic DNA fragmentation. In contrast, cisplatin

Gland Surg
VOL-11 NO 1 (2026)
ISSN:2227-684X | E-ISSN:2227-8575

predominantly increased the sub-G1 cell population in both cell lines. These findings are consistent with studies on Fucus vesiculosus fucoidan, which induced G1 arrest in A549 cells through p21 upregulation and PI3K inhibition, as well as with Sargassum muticum extracts, which caused G1 or G2/M arrest depending on the cell type (El-Seedi *et al*., 2025). Conceptually, PP's ability of PP to halt proliferation at the G1 phase reflects a regulatory checkpoint intervention, in contrast to cisplatin's abrupt genotoxic effects.

In parallel, gene expression analysis further corroborated these findings. In A549 cells, PP upregulated Bax and downregulated Bcl-2, PI3K, and AKT1, thereby confirming the activation of intrinsic apoptosis and suppression of survival signaling. In MCF-7 cells, Bax levels remained unchanged; however, Bcl-2 and AKT1 levels were reduced, whereas PI3K was paradoxically upregulated, suggesting compensatory survival signaling. These results align with reports indicating that brown algal extracts modulate Bax/Bcl-2 ratios and inhibit PI3K/AKT signaling, while also highlighting cell line-specific differences in pathway engagement (Catarino *et al*., 2021).

The modulation of Bax, Bcl-2, PI3K, and AKT1 expression observed in our study is consistent with existing evidence that *Padina pavonica* and related marine extracts influence the apoptotic and survival signaling pathways of different cancer types (Awaji et al., 2025). Holz *et al*. (2023) demonstrated that the combined inhibition of Bcl-2 and PI3K/AKT signaling synergistically promotes apoptosis in leukemia cells, underscoring the therapeutic relevance of targeting these pathways. Additionally, analyses of the Bcl-2 protein family highlight their crucial involvement in controlling apoptosis and indicate that irregular expression patterns are significant markers of cancer development (Liu *et al*., 2022). Together, these investigations support our conclusion that *P. pavonica* acts as a multi-targeted modulator, simultaneously interrupting pro-survival pathways and promoting pro-apoptotic activities.

The downregulation of Bcl-2, PI3K, and AKT1 expression in A549 lung adenocarcinoma and MCF7 breast adenocarcinoma cells after *Padina pavonica* extract treatment shows the ability of seaweed to modulate pathways governing cell survival and apoptosis. Bcl-2, an anti-apoptotic protein that maintains mitochondrial membrane integrity, is suppressed, facilitating cytochrome c release and caspase cascade activation, leading to cell death. The inhibition of PI3K and AKT1 disrupts downstream molecules, including mTOR and GSK-3β, attenuating proliferative signals and enhancing apoptosis. This targeting of both the apoptotic machinery and pro-survival signaling represents a multifaceted approach, as the PI3K/AKT pathway is frequently hyperactivated in lung and breast cancers, contributing to uncontrolled proliferation. The dose-dependent reduction in Bcl-2, PI3K, and AKT1 expression aligns with studies showing that marine algal extracts exert anticancer effects through similar mechanisms (El-Din et al., 2016; Khanavi et al., 2012). The selective suppression of oncogenic markers in A549 and MCF7 cell lines demonstrates *the potential of P. pavonica* as a source of bioactive therapeutic compounds. MCF7 cells showed pronounced sensitivity to Padina pavonica-induced apoptosis, likely due to interactions between estrogen receptor signaling and the PI3K/AKT pathway, where Bcl-2 downregulation may occur through ER-mediated repression. A549 cells showed significant PI3K/AKT inhibition, consistent with the role of this pathway in lung carcinogenesis. The underlying molecular mechanisms involve induction of oxidative stress and modulation of receptor tyrosine kinases. The downregulation of Bcl-2, PI3K, and AKT1 suggests a synergistic potential when combined with standard treatments. These findings support marine macroalgae as promising sources

Gland Surg
VOL-11 NO 1 (2026)
ISSN:2227-684X | E-ISSN:2227-8575

of novel anticancer agents, warranting further investigation into their active constituents and in vivo validation (Vijayabaskar et al., 2012; Wang et al., 2018; Manojlovic et al., 2010).

Our results suggest that P. *pavonica* extract is a multi-targeted anticancer agent. In A549 cells, it acts through mitochondrial apoptosis and PI3K/AKT suppression, while in MCF-7 cells, it engages alternative pathways to overcome apoptotic resistance. Compared to cisplatin, PP gradually destabilizes the survival architecture through layered biochemical interventions, reflecting the ecological resilience of marine algae-robust yet adaptive-in cancer modulation.

Future directions should focus on the need for the exploration of upstream regulators (cyclin D/CDK4/6, p21), and assessment of selectivity in non-tumorigenic cells to evaluate the therapeutic window. Nonetheless, the present findings provide strong evidence that *Padina pavonica* extract exerts anticancer activity through apoptosis induction, cell cycle disruption, and survival pathway modulation, situating it within the broader active brown algal extracts.

5. Conclusion

In summary, this study revealed that the ethanol extract of *Padina pavonica* (PP) exhibits notable anticancer effects in human lung (A549) and breast (MCF-7) cancer cells. The extract decreased cell viability in a dose-dependent fashion, caused specific morphological changes, and initiated apoptosis mainly through late apoptotic processes. Importantly, treatment with PP led to G1-phase arrest in A549 cells and sub-G1 accumulation in MCF-7 cells, suggesting interference with the cell cycle. Mechanistically, the extract influenced crucial apoptotic regulators by increasing Bax and decreasing Bcl-2, while also inhibiting the PI3K/AKT survival pathway at both the gene and protein levels. Additionally, PP treatment reduced intracellular glutathione and lowered the total antioxidant capacity, indicating that oxidative stress plays a role in its cytotoxic effects. Although less effective than cisplatin, *the P. pavonica* extract demonstrated a multi-faceted approach, targeting redox imbalance, apoptotic signaling, and survival pathway inhibition, rather than causing direct genotoxic damage. These results highlight the potential of *Padina pavonica* as a source of bioactive compounds with anticancer capabilities and emphasize the promise of marine brown algae for further phytochemical and pharmacological research. Future investigations should concentrate on isolating compounds, validating their effects in vivo, and evaluating their selectivity towards normal cells to enhance their translational significance.

6. References

- Abuwatfa, W. H., Pitt, W. G., & Husseini, G. A. (2024). Scaffold-based 3D cell culture models in cancer research. *Journal of Biomedical Science*, *31*(1), 7.
- Awaji, A. A., Alhamdi, H. W., Alshehri, K. M., Alfaifi, M. Y., Shati, A. A., Elbehairi, S. E. I., Radwan, N. A.-F., Hafez, H. S., Elshaarawy, R. F. M., & Welson, M. (2025). Bio-molecular Fe(III) and Zn(II) complexes stimulate the interplay between PI3K/AKT1/EGFR inhibition and induce autophagy and apoptosis in epidermal skin cell cancer. *Journal of Inorganic Biochemistry*, *262*, 112720. https://doi.org/https://doi.org/10.1016/j.jinorgbio.2024.112720
- Bernardini, G., Minetti, M., Polizzotto, G., Biazzo, M., & Santucci, A. (2018). Pro-Apoptotic Activity of French Polynesian Padina pavonica Extract on Human Osteosarcoma Cells. In *Marine Drugs* (Vol. 16, Issue 12, p. 504). https://doi.org/10.3390/md16120504
- Catarino, M. D., Amarante, S. J., Mateus, N., Silva, A. M. S., & Cardoso, S. M. (2021). Brown

Algae Phlorotannins: A Marine Alternative to Break the Oxidative Stress, Inflammation and Cancer Network. In *Foods* (Vol. 10, Issue 7, p. 1478). https://doi.org/10.3390/foods10071478

- Dasari, S., & Bernard Tchounwou, P. (2014). Cisplatin in cancer therapy: Molecular mechanisms of action. *European Journal of Pharmacology*, *740*, 364–378. https://doi.org/https://doi.org/10.1016/j.ejphar.2014.07.025
- de Martel, C., Georges, D., Bray, F., Ferlay, J., & Clifford, G. M. (2020). Global burden of cancer attributable to infections in 2018: a worldwide incidence analysis. *The Lancet Global Health*, *8*(2), e180–e190. https://doi.org/10.1016/S2214-109X(19)30488-7
- El-Seedi, H. R., Refaey, M. S., Elias, N., El-Mallah, M. F., Albaqami, F. M. K., Dergaa, I., Du, M., Salem, M. F., Tahir, H. E., Dagliaa, M., Yosri, N., Zhang, H., El-Seedi, A. H., Guo, Z., & Khalifa, S. A. M. (2025). Marine natural products as a source of novel anticancer drugs: an updated review (2019–2023). *Natural Products and Bioprospecting*, *15*(1), 13. https://doi.org/10.1007/s13659-024-00493-5
- Elmorsy, E. A., Saber, S., Hamad, R. S., Abdel-Reheim, M. A., El-kott, A. F., AlShehri, M. A., Morsy, K., Salama, S. A., & Youssef, M. E. (2024). Advances in understanding cisplatin-induced toxicity: Molecular mechanisms and protective strategies. *European Journal of Pharmaceutical Sciences*, *203*, 106939. https://doi.org/https://doi.org/10.1016/j.ejps.2024.106939
- Galluzzi, L., Senovilla, L., Vitale, I., Michels, J., Martins, I., Kepp, O., Castedo, M., & Kroemer, G. (2012). Molecular mechanisms of cisplatin resistance. *Oncogene*, *31*(15), 1869–1883. https://doi.org/10.1038/onc.2011.384
- Giaquinto, A. N., Sung, H., Miller, K. D., Kramer, J. L., Newman, L. A., Minihan, A., Jemal, A., & Siegel, R. L. (2022). Breast Cancer Statistics, 2022. *CA: A Cancer Journal for Clinicians*, *72*(6), 524–541. https://doi.org/10.3322/caac.21754
- Górska, S., Maksymiuk, A., & Turło, J. (2021). Selenium-Containing Polysaccharides—Structural Diversity, Biosynthesis, Chemical Modifications and Biological Activity. In *Applied Sciences* (Vol. 11, Issue 8, p. 3717). https://doi.org/10.3390/app11083717
- Holz, C., Lange, S., Sekora, A., Knuebel, G., Krohn, S., Murua Escobar, H., Junghanss, C., & Richter, A. (2023). Combined BCL-2 and PI3K/AKT Pathway Inhibition in KMT2A-Rearranged Acute B-Lymphoblastic Leukemia Cells. In *International Journal of Molecular Sciences* (Vol. 24, Issue 2, p. 1359). https://doi.org/10.3390/ijms24021359
- Jerković, I., Kranjac, M., Marijanović, Z., Roje, M., & Jokić, S. (2019). Chemical Diversity of Headspace and Volatile Oil Composition of Two Brown Algae (Taonia atomaria and Padina pavonica) from the Adriatic Sea. In *Molecules* (Vol. 24, Issue 3, p. 495). https://doi.org/10.3390/molecules24030495
- Jin, J.-O., Yadav, D., Madhwani, K., Puranik, N., Chavda, V., & Song, M. (2022). Seaweeds in the Oncology Arena: Anti-Cancer Potential of Fucoidan as a Drug—A Review. In *Molecules* (Vol. 27, Issue 18, p. 6032). https://doi.org/10.3390/molecules27186032
- Kalinina, E. (2024). Glutathione-dependent pathways in cancer cells. *International Journal of Molecular Sciences*, *25*(15), 8423.
- Kim, J., Harper, A., McCormack, V., Sung, H., Houssami, N., Morgan, E., Mutebi, M.,

Gland Surg
VOL-11 NO 1 (2026)
ISSN:2227-684X | E-ISSN:2227-8575

Garvey, G., Soerjomataram, I., & Fidler-Benaoudia, M. M. (2025). Global patterns and trends in breast cancer incidence and mortality across 185 countries. *Nature Medicine*, *31*(4), 1154–1162. https://doi.org/10.1038/s41591-025-03502-3

- Kouroshnia, A., Zeinali, S., Irani, S., & Sadeghi, A. (2022). Induction of apoptosis and cell cycle arrest in colorectal cancer cells by novel anticancer metabolites of Streptomyces sp. 801. *Cancer Cell International*, *22*(1), 235. https://doi.org/10.1186/s12935-022-02656-1
- Lee, H., Kim, J.-S., & Kim, E. (2012). Fucoidan from Seaweed Fucus vesiculosus Inhibits Migration and Invasion of Human Lung Cancer Cell via PI3K-Akt-mTOR Pathways. *PLOS ONE*, *7*(11), e50624.
- Li, X., Chen, L., Yan, Z., Xu, T., & Zhao, Y. (2025). Triptonide suppresses the FOXK1/AKT2 axis to reverse malignant phenotype and improve cisplatin efficacy in esophageal squamous cell carcinoma. *Genes & Genomics*. https://doi.org/10.1007/s13258-025-01701-3
- Liu, S., Qiao, X., Wu, S., Gai, Y., Su, Y., Edwards, H., Wang, Y., Lin, H., Taub, J. W., Wang, G., & Ge, Y. (2022). c-Myc plays a critical role in the antileukemic activity of the Mcl-1-selective inhibitor AZD5991 in acute myeloid leukemia. *Apoptosis*, *27*(11), 913–928. https://doi.org/10.1007/s10495-022-01756-7
- Luo, B., Wang, Z., Chen, J., Chen, X., Li, J., Li, Y., Li, R., Liu, X., Song, B., Cheong, K.-L., & Zhong, S. (2023). Physicochemical Characterization and Antitumor Activity of Fucoidan and Its Degraded Products from Sargassum hemiphyllum (Turner) C. Agardh. In *Molecules* (Vol. 28, Issue 6, p. 2610). https://doi.org/10.3390/molecules28062610
- Mahmood, T., & Yang, P.-C. (2012). Western blot: technique, theory, and trouble shooting. *North American Journal of Medical Sciences*, *4*(9), 429–434. https://doi.org/10.4103/1947-2714.100998
- Makhlof, M. E. M., El-Sheekh, M. M., & EL-Sayed, A. I. M. (2024). In vitro antibiofilm, antibacterial, antioxidant, and antitumor activities of the brown alga Padina pavonica biomass extract. *International Journal of Environmental Health Research*, *34*(4), 1861–1878. https://doi.org/10.1080/09603123.2023.2165045
- McDonald, J. H. (2014). *Handbook of biological statistics*.
- Muñoz-Losada, K. J., Gallego-Villada, M., & Puertas-Mejía, M. A. (2025). An Overview of Sargassum Seaweed as Natural Anticancer Therapy. In *Future Pharmacology* (Vol. 5, Issue 1, p. 5). https://doi.org/10.3390/futurepharmacol5010005
- Namvar, F., Mohamad, R., Baharara, J., Zafar-Balanejad, S., Fargahi, F., & Rahman, H. S. (2013). Antioxidant, Antiproliferative, and Antiangiogenesis Effects of Polyphenol-Rich Seaweed (Sargassum muticum). *BioMed Research International*, *2013*(1), 604787. https://doi.org/https://doi.org/10.1155/2013/604787
- Palpperumal, S., Sankaralingam, S., Balachandran, C., Mahendran, S., Venkatesh, S., Alharbi, N. S., Thiruvengadam, M., Duraipandiyan, V., & Baskar, K. (2024). Antioxidant, Anticancer, Hepatoprotective and Wound Healing Activity of Fucopyranose (Sulfated Polysaccharides) from Padina pavonica (L.). *Indian Journal of Microbiology*, *64*(4), 1805–1825. https://doi.org/10.1007/s12088-024-01237-2
- Pradhan, B., Bhuyan, P. P., & Ki, J.-S. (2023). Immunomodulatory, Antioxidant, Anticancer,

and Pharmacokinetic Activity of Ulvan, a Seaweed-Derived Sulfated Polysaccharide: An Updated Comprehensive Review. In *Marine Drugs* (Vol. 21, Issue 5). https://doi.org/10.3390/md21050300

- Sali, R., Jiang, Y., Attaranzadeh, A., Holmes, B., & Li, R. (2024). Morphological diversity of cancer cells predicts prognosis across tumor types. *JNCI: Journal of the National Cancer Institute*, *116*(4), 555–564.
- Santhanam, R. C., Ali, S., Yacoob, M., & Venkatraman, A. (2013). *Invitro cytotoxicity assay of Fucoidan extracted from Turbinaria conoides against cancer cell lines MCF7 , A549 , and normal cell line L929*. 1–6.
- Santhanam, R. C., Yacoob, S. A. M., Rathinam, R., & Sirisha, D. R. (2024). *Isolation of Fucoidan from seaweed Turbinaria conoides and evaluation of its anticancer potential on animal models*.
- Shahin, A., Nabil-Adam, A., Elnagar, K., Osman, H., & Shreadah, M. A. (2022). Bioactivity and metabolomics fingerprinting characterization of different organic solvents extracts of Padina pavonica collected from Abu Qir Bay, Egypt. *Egyptian Journal of Chemistry*, *65*(12), 207–225.
- Silvestrini, A., Meucci, E., Ricerca, B. M., & Mancini, A. (2023). Total antioxidant capacity: biochemical aspects and clinical significance. *International Journal of Molecular Sciences*, *24*(13), 10978.
- Sudha, G., & Balasundaram, A. (2018). Determination of Bioactive Components in the Methanolic Extract of Padina pavonica Using GC-MS. *World J. Pharm. Res*, *7*, 991–997.
- Sung, H., Ferlay, J., Siegel, R. L., Laversanne, M., Soerjomataram, I., Jemal, A., & Bray, F. (2021). Global Cancer Statistics 2020: GLOBOCAN Estimates of Incidence and Mortality Worldwide for 36 Cancers in 185 Countries. *CA: A Cancer Journal for Clinicians*, *71*(3), 209–249. https://doi.org/https://doi.org/10.3322/caac.21660
- Tamzi, N. N., Rahman, M. M., & Das, S. (2024). Recent Advances in Marine-Derived Bioactives Towards Cancer Therapy. In *International Journal of Translational Medicine* (Vol. 4, Issue 4, pp. 740–781). https://doi.org/10.3390/ijtm4040051
- Wang, H., Li, Y., Li, C., Liu, X., Liu, B., Wu, C., & Zeng, F. (2025). Anticancer effects of Sargassum pallidum polysaccharide through the modulation of ROS-mediated signaling pathways. *International Journal of Biological Macromolecules*, *318*, 145026. https://doi.org/https://doi.org/10.1016/j.ijbiomac.2025.145026
- Yang, X.-H., Sladek, T. L., Liu, X., Butler, B. R., Froelich, C. J., & Thor, A. D. (2001). Reconstitution of Caspase 3 Sensitizes MCF-7 Breast Cancer Cells to Doxorubicin- and Etoposide-induced Apoptosis1. *Cancer Research*, *61*(1), 348–354.
- Yılmaz, S., Doğanyiğit, Z., Oflamaz, A. O., Ateş, Ş., Söylemez, E. S. A., Nisari, M., & Farooqı, A. A. (2023). Determination of Rutin's antitumoral effect on EAC solid tumor by AgNOR count and PI3K/AKT/mTOR signaling pathway. *Medical Oncology*, *40*(5), 131. https://doi.org/10.1007/s12032-023-01999-7